

## N O T I C E

THIS DOCUMENT HAS BEEN REPRODUCED FROM  
MICROFICHE. ALTHOUGH IT IS RECOGNIZED THAT  
CERTAIN PORTIONS ARE ILLEGIBLE, IT IS BEING RELEASED  
IN THE INTEREST OF MAKING AVAILABLE AS MUCH  
INFORMATION AS POSSIBLE

DOE/NASA/1028-29  
NASA TM-81674

# Effects of Mistuning on Bending-Torsion Flutter and Response of a Cascade in Incompressible Flow

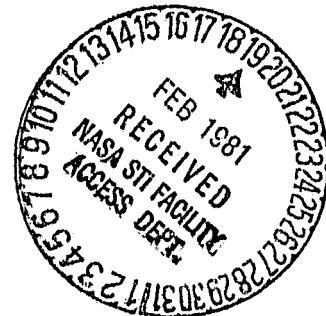
(NASA-TM-81674) EFFECTS OF MISTUNING ON  
BENDING-TORSION FLUTTER AND RESPONSE OF A  
CASCADE IN INCOMPRESSIBLE FLOW (NASA) 20 p  
HC A02/MF A01 CSCL 20K

N81-16494

Unclas  
G3/39 41294

Krishna Rao V. Kaza  
The University of Toledo  
and

Robert E. Kielb  
National Aeronautics and Space Administration  
Lewis Research Center



Work performed for  
**U.S. DEPARTMENT OF ENERGY**  
**Conservation and Solar Energy**  
**Division of Solar Thermal Energy Systems**

Prepared for  
Dynamics Specialists Conference sponsored by the  
American Institute of Aeronautics and Astronautics  
Atlanta, Georgia, April 9-11, 1981

#### NOTICE

This report was prepared to document work sponsored by the United States Government. Neither the United States nor its agent, the United States Department of Energy, nor any Federal employees, nor any of their contractors, subcontractors or their employees, makes any warranty, express or implied, or assumes any legal liability or responsibility for the accuracy, completeness, or usefulness of any information, apparatus, product or process disclosed, or represents that its use would not infringe privately owned rights.

# **Effects of Mistuning on Bending-Torsion Flutter and Response of a Cascade in Incompressible Flow**

Krishna Rao V. Kaza  
The University of Toledo  
Toledo, Ohio 43606

and

Robert E. Kielb  
National Aeronautics and Space Administration  
Lewis Research Center  
Cleveland, Ohio 44135

Work performed for  
U.S. DEPARTMENT OF ENERGY  
Conservation and Solar Energy  
Division of Solar Thermal Energy Systems  
Washington, D.C. 20545  
Under Interagency Agreement EX-76-I-01-1028

Prepared for  
Dynamics Specialists Conference sponsored by the  
American Institute of Aeronautics and Astronautics  
Atlanta, Georgia, April 9-11, 1981

EFFECTS OF MISTUNING ON BENDING-TORSION FLUTTER AND RESPONSE OF A CASCADE IN INCOMPRESSIBLE FLOW

by

Krishna Rao V. Kaza\*  
The University of Toledo and

National Aeronautics and Space Administration  
Lewis Research Center  
Cleveland, Ohio 44135

and

Robert E. Kielb\*\*  
National Aeronautics and Space Administration  
Lewis Research Center  
Cleveland, Ohio 44135

Abstract

This paper presents an investigation of the effects of blade mistuning on the aeroelastic stability and response of a cascade in incompressible flow. The aerodynamic, inertial, and structural coupling between the bending and torsional motions of each blade and the aerodynamic coupling between the blades are included in the formulation. A digital computer program was developed to conduct parametric studies. Results indicate that the mistuning has a beneficial effect on the coupled bending-torsion and uncoupled torsion flutter. The effect of mistuning on forced response, however, may be either beneficial or adverse, depending on the engine order of the forcing function. Additionally, the results illustrate that it may be feasible to utilize mistuning as a passive control to increase flutter speed while maintaining forced response at an acceptable level.

Nomenclature

[A] aerodynamic matrix due to motion  
[A<sub>r</sub>] aerodynamic matrix due to motion in rth mode; r = 0, 1, 2 ... N-1  
{AD} aerodynamic matrix due to wake induced flow  
{AD<sub>r</sub>} aerodynamic matrix due to wake induced flow in the rth mode, r = 0, 1, 2 ... N-1  
a elastic axis location, nondimensional  
b semichord  
c chord  
[D],[D<sub>s</sub>] matrices defined in equation (11); s = 0, 1, 2 ... N-1  
[E] matrix defined in equation (4)  
E(s,r) defined in equation (4)

e base for natural logarithm  
[G],[G<sub>s</sub>] matrices defined in equation (11); s = 0, 1, 2 ... N-1  
G<sub>Kh<sub>s</sub></sub>, G<sub>Kα<sub>s</sub></sub> quantities defined in equation (11)  
h<sub>s</sub> bending deflection of sth blade  
h<sub>ar</sub> bending deflection of blade in rth mode of tuned cascade  
[I] unit matrix  
I<sub>α<sub>s</sub></sub> mass moment of inertia of sth blade about elastic axis per unit span; (=m<sub>s</sub>r<sub>α<sub>s</sub></sub><sup>2</sup>b<sup>2</sup>)  
i √-1  
K<sub>h<sub>s</sub></sub>, K<sub>α<sub>s</sub></sub> bending and torsional stiffness respectively, of sth blade  
k reduced frequency, ωb/V  
k<sub>F</sub> reduced flutter frequency, ω<sub>F</sub>b/V<sub>F</sub>  
L<sub>s</sub><sup>M</sup> lift due to motion of sth blade per unit span, positive up  
L<sub>s</sub><sup>W</sup> lift due to wakes of sth blade per unit span, positive up  
l<sub>h<sub>ar</sub></sub>, l<sub>α<sub>ar</sub></sub> nondimensional lift coefficients due to bending and torsional motions, respectively, in rth mode  
l<sub>α<sub>hr</sub></sub>, l<sub>α<sub>ar</sub></sub> nondimensional moment coefficient due to bending and torsional motion, respectively, in rth mode  
l<sub>w<sub>hr</sub></sub>, l<sub>w<sub>ar</sub></sub> nondimensional lift and moment coefficients, respectively, due to wake in rth mode  
M<sub>s</sub><sup>M</sup> moment about the elastic axis due to motion of sth blade per unit span, positive nose up  
M<sub>s</sub><sup>W</sup> moment of sth blade per unit span about the elastic axis due to wake, positive nose up

E-699

\*Adjunct Professor, Mechanical Engineering Department, Member AIAA.  
\*\*Aerospace Engineer, Structures Branch, Member ASME.

$m_B$	mass per unit span of sth blade	$\theta_B$	azimuthal position of sth blade, defined in equation (6)
$N$	number of blades in cascade	$\mu_B$	mass coefficient of sth blade, $m_B/\rho b^2$
$[P]$	matrix defined in equation (11)	$\bar{\mu}$	real part of eigenvalue, defined in equation (12)
$q_{her}, q_{har}$	multiblade coordinates for bending motion in rth mode	$\bar{\nu}$	imaginary part of eigenvalue, defined in equation (12)
$q_{acr}, q_{aar}$	multiblade coordinates for torsional motion in rth mode	$\bar{\nu}_F$	nondimensional flutter frequency
$r$	integer specifying the mode of tuned rotor; $r = 0, 1, 2 \dots N-1$ ; also the engine order of the excitation	$\xi$	stagger angle, figure 1
$r_{\alpha_B}$	radius of gyration of sth blade, nondimensionalized with respect to $b$	$\rho$	fluid density
$s$	integer specifying blade, $s = 0, 1, 2 \dots N-1$ ; also blade spacing (fig. 1)	$\omega$	frequency
$S_{\alpha_B}$	static mass moment of sth blade per unit span about elastic axis, positive when center of gravity is aft of elastic axis	$\omega_0$	reference frequency
$t$	time	$\omega_{h_B}$	$\sqrt{K_{h_B}/m_B}$
$V$	freestream velocity relative to the blade	$\omega_{\alpha_B}$	$\sqrt{K_{\alpha_B}/I_{\alpha_B}}$
$V_F$	flutter speed	$[ ], [ ]$	matrices
$w_r$	velocity induced by wakes	$(\dot{\quad})$	differentiation with time
$\{X\}$	column matrix, defined in equation (4)	$[ ]^{-1}$	inverse of a matrix
$X, Z$	rectangular coordinate axes	$\sum$	indicate summation over $r = 0, 1, 2 \dots N-1$
$x_{\alpha_B}$	dimensionless static unbalance of sth blade ( $=S_{\alpha_B}/m_B b$ )		
$\{Y\}$	column matrix, defined in equation (4)		
$\alpha_B$	amplitude of torsional motion of sth blade, positive clockwise		
$\alpha_{B, id}$	torsional amplitude of each blade of tuned rotor		
$\alpha_{ar}$	amplitude of torsional deflection of a blade in rth mode of a tuned cascade		
$\beta_r$	interblade phase angle, $2\pi r/N$		
$\gamma$	nondimensional eigenvalue, $(\omega_0/\omega)^2$		
$\gamma_{h_B}$	nondimensional uncoupled bending frequency of sth blade		
$\gamma_{\alpha_B}$	nondimensional uncoupled torsional frequency of sth blade		
$\delta_{h_B}, \delta_{\alpha_B}$	logarithmic decrements of sth blade in bending and torsion, respectively		
$\zeta_{h_B}, \zeta_{\alpha_B}$	damping ratios of sth blade in bending and torsion, respectively		
$\eta$	location of elastic axis measured from leading edge, $(a + 1)/2$		

## I. Introduction

In the development of modern aircraft turboprop engines, the aeroelastic stability and response of bladed-disk assemblies have been among the most difficult problems encountered. The study of stability and response in these assemblies is complicated by the presence of small differences between the individual blades, known as mistuning. The published results in this area which will be discussed later have shown that mistuning can have a beneficial effect on turbine engine blade flutter and an adverse effect on forced response. Experience<sup>(1,2)</sup> has further shown that there have been costly failures in the development and production phases in which mistuning appeared to have played an important role. Thus, an improved basic understanding of these effects is important in the design phase.

To improve the basic understanding of the effects of mistuning on aeroelastic stability and response and then to explore the possibility of utilizing mistuning as a passive control to alleviate flutter and to minimize forced response, an effort has been in progress in the Structural Dynamics Section, NASA Lewis Research Center. As a part of this general effort, the effects of mistuning on coupled bending-torsion flutter and on aeroelastic response due to wakes have been studied. This paper presents the results of the study for incompressible flow.

Either because of the complexities or because of the general belief that the turbomachinery blade

flutter involves only a single degree of freedom, previous researchers<sup>(2-7)</sup> have studied the effect of blade mistuning on aeroelastic stability and response by considering either pure bending motion or pure torsional motion of the blades. The studies of multi-degree of freedom blade flutter in the published literature<sup>(5,8,9,10,11)</sup> have been limited to tuned cascades. To the best of the authors' knowledge, the forced response of both tuned and mistuned cascades using multi-degree freedom models has not been presented in the published literature. Thus, the problem considered in this paper is a logical extension to the present state of the literature on flutter and forced response of blades with mistuning.

The mathematical model considered herein is of the discretized, lumped parameter type, utilizing discrete masses, mass moment of inertia, and linear and rotational springs to represent the individual blades. The unsteady aerodynamic loads were calculated by using Whitehead's<sup>(12)</sup> incompressible flow cascade theory. Thus, the model considered is simple enough to be used for extensive parametric studies. At the same time, it is adequate to represent the basic dynamic characteristics of a mistuned cascade, to provide guidance in refining both the aerodynamic and structural models, and to check the results obtained from finite element formulations, such as one presented in reference 13. Recently, the authors have extended the present work into the subsonic and supersonic flow regimes in reference 14.

## II. Theory

In general, the components which comprise a bladed-disk system have complex geometries. The analysis of this complex system, as stated earlier, is further complicated by blade mistuning. To accomplish the stated objectives of the paper, it is necessary to develop a model which simplifies the analysis, yet maintains the basic dynamic characteristics. For this reason only two degrees of freedom (one bending and one torsion) for each blade are considered in this paper. However, the authors have plans to add additional blade degrees of freedom and disk flexibilities in addition to other refinements to the present model. The general motion of a mistuned cascade is assumed to be a combination of all possible motions of the associated tuned cascade. It will, therefore, be instructive first to develop and understand the model of a tuned cascade.

### A. Tuned Cascade Model

The geometry of a tuned cascade model is shown in figure 1. The disk is assumed to be rigid and the bladed assembly is modeled as infinite two-dimensional cascade of airfoils in a uniform upstream flow with a velocity  $V$  as illustrated in figure 1. The effects of wakes shed from upstream obstructions are included. The wakes considered are limited to sinusoidal distortions represented by vorticity perturbation, so that they are convected downstream at the flow velocity  $V$ . The amplitude of the wakes is specified by the velocity which the wakes would induce at the position of the mid-chord point of the reference blade as indicated in

figure 1. The motion of the airfoils in each mode of the tuned cascade is assumed to be simple harmonic with a constant phase angle  $\beta_r$  between adjacent blades. Also, this interblade phase angle is restricted by Lamb's<sup>(15)</sup> assumption to the  $N$  discrete values  $\beta_r = 2\pi r/N$  where  $r = 0, 1, 2, \dots, N-1$ . Consequently, there are  $N$  modes for the cascade with each blade having the same amplitude. The motion of a tuned cascade in  $r$ th mode involving bending and torsion coupling can be represented in the form of a traveling wave as shown in figure 1. The motion of the  $s$ th blade when the cascade vibrates in the  $r$ th mode is indicated in figure 2. For a tuned system, the modes with different interblade phase angles are uncoupled and hence one can write

$$\begin{Bmatrix} h_B \\ \alpha_B \end{Bmatrix} e^{i\omega t} = \begin{Bmatrix} h_{ar} \\ \alpha_{ar} \end{Bmatrix} e^{i(\omega t + \beta_r s)} \quad (1)$$

Furthermore, it is adequate to analyze the motion of a single blade in each of the interblade phase angle modes separately. Hence, the number of degrees of freedom of a tuned cascade for the present case is reduced to two for each value of  $\beta_r$ .

### B. Mistuned Cascade Model

In a randomly mistuned cascade, the blades are not identical and can have different response amplitudes. In addition, the phase angle between adjacent blades can vary. Because of the spatial periodicity, the general motion of a blade in a mistuned cascade can be expressed as a combination of the motions in all possible interblade phase angle modes of the corresponding tuned cascade. Consequently, the motion of the  $s$ th blade can be written in the traveling wave form

$$\begin{Bmatrix} h_B \\ \alpha_B \end{Bmatrix} e^{i\omega t} = \sum_{r=0}^{N-1} \begin{Bmatrix} h_{ar} \\ \alpha_{ar} \end{Bmatrix} e^{i(\omega t + \beta_r s)} \quad (2)$$

The quantities  $h_{ar}$ 's and  $\alpha_{ar}$ 's were called as the 'aerodynamic modes' in reference 4. For a cascade with  $N$  mistuned blades, equation (2) can be generalized as

$$\{X\} e^{i\omega t} = [E]\{Y\} e^{i\omega t} \quad (3)$$

where

$$\{X\} = \begin{Bmatrix} h_0 \\ \alpha_0 \\ \vdots \\ h_{N-1} \\ \alpha_{N-1} \end{Bmatrix} \quad \{Y\} = \begin{Bmatrix} h_{a0} \\ \alpha_{a0} \\ \vdots \\ h_{a(N-1)} \\ \alpha_{a(N-1)} \end{Bmatrix} \quad (4)$$

'cont'd.

$$[E] = \begin{bmatrix} E(0,0) & 0 & E(0,1) & 0 & \dots \\ 0 & E(0,0) & 0 & E(0,1) & \dots \\ E(1,0) & 0 & \dots & & \\ 0 & E(1,0) & \dots & & \\ \vdots & \vdots & & & \\ \vdots & \vdots & & E(N-1,N-1) & 0 \\ \vdots & \vdots & & 0 & E(N-1,N-1) \end{bmatrix}$$

$$E(\theta, r) = c \frac{2\pi i \alpha r}{N} \quad (4)$$

(cont.)

It should be remarked that the motion of a blade in a cascade with and without mistuning can also be expressed in a standing wave form. Since the stability and response are independent of the form used, consideration of either of these forms is adequate to describe the motion. In most of the published literature on flutter analysis of bladed-disk assemblies, the traveling wave form is preferred. This is in contrast to the conventional flutter analysis of a fixed wing aircraft in which the standing wave form is generally used. The motion of the  $s$ th blade of a mistuned rotor in the standing wave form may be written as

$$\begin{Bmatrix} h_B \\ \alpha_B \end{Bmatrix} e^{i\omega t} = \sum_{r=0}^{N-1} \begin{Bmatrix} q(t) \cos \theta_B r + q(t) \sin \theta_B r \\ h_{Br} \\ q(t) \cos \theta_B r + q(t) \sin \theta_B r \\ \alpha_{Br} \end{Bmatrix} \quad (5)$$

where

$$\theta_B = \beta r s / r \quad (6)$$

It is of interest to note that the special cases of the form given by equation (5) are known as 'multi-blade coordinate transformations' in the literature dealing with the helicopter and prop-rotor aeroelasticity. This transformation has certain advantages in the analyses, particularly when the coupling between the rotor and supporting structure are involved, and when the coefficients in the equations of motion are periodic in time. Hence, the standing wave representation may be expected to have similar advantages if the analysis includes bearing motion, whirling motion of shaft, stand motion, etc. An interesting discussion on both traveling and standing wave representations for tuned bladed disk assemblies is presented in reference 16.

### C. Structural Model

The structural model of the  $s$ th blade of a mistuned cascade is illustrated in figure 2. Each airfoil is suspended by bending and torsional springs,  $K_{h_B}$  and  $K_{\alpha_B}$ , respectively. The airfoil

is assumed to be rigid in the chordwise direction, and this motion is neglected. The elastic coupling between bending and torsion due to pretwist, shrouds, and rotation of the rotor is modeled through the offset distance ( $b_{xy}$ ) between the center of gravity and elastic axis. The centrifugal stiffening effects due to rotation are included in the bending and torsional spring constants. The elastic and dynamic properties of the blades are represented by their respective values at the three-quarters station of blade span. This model may be viewed as a logical extension of the so-called 'typical section wing' used in fixed wing aeroelasticity. (17)

### D. Aerodynamic Model

The unsteady aerodynamic loads were calculated by using Whithead's (12) cascade theory in the incompressible unsteady flow. This theory is an extension of two-dimensional unsteady airfoil theory of Theoderson to account for cascade effects. The effect of airfoil thickness, camber, and  $v'$  dy state angle of attack are neglected. As mentioned earlier, the effects of wakes from a periodic obstruction upstream are included in the form of a vorticity perturbation. It should be noted that the direction of the velocity, as shown in figure 1, induced by the wakes is opposite to that of reference 12. In view of the basic objectives of this paper, it is felt that this incompressible theory is adequate. However, the compressibility effects will be included by using Smith's (18) theory in the subsonic flow regime, and Adamczyk and Goldstein's (19) theory in the supersonic flow regime. These results will be reported in reference 14.

### E. Equations of Motion

A simple application of Lagrange's equation to the mathematical model of the  $s$ th blade in figure 2 leads to the following coupled bending-torsion equations

$$\begin{bmatrix} m_B & S_{\alpha_B} \\ S_{\alpha_B} & I_{\alpha_B} \end{bmatrix} \begin{Bmatrix} \frac{d^2}{dt^2} (h_B e^{i\omega t}) \\ \frac{d^2}{dt^2} (\alpha_B e^{i\omega t}) \end{Bmatrix} + \begin{bmatrix} (1 + 2i\zeta_{h_B}) m_B \omega^2 & 0 \\ 0 & (1 + 2i\zeta_{\alpha_B}) I_{\alpha_B} \omega^2 \end{bmatrix} \begin{Bmatrix} h_B e^{i\omega t} \\ \alpha_B e^{i\omega t} \end{Bmatrix} = \begin{Bmatrix} -L_B^M - L_B^W \\ M_B^M + M_B^W \end{Bmatrix} \quad (7)$$

Structural damping is added to the equations of motion by multiplying the uncoupled stiffness coefficients in the bending and torsion by  $(1 + 2i\zeta_{h_B})$  and  $(1 + 2i\zeta_{\alpha_B})$ , respectively. The critical damping

ratios,  $\zeta_{h_B}$  and  $\zeta_{\alpha_B}$ , are related to the logarithmic decrements,  $\delta_{h_B}$  and  $\delta_{\alpha_B}$ , by the relation  $\delta_{h_B} = 2\pi\zeta_{h_B}$  and  $\delta_{\alpha_B} = 2\pi\zeta_{\alpha_B}$ . The aerodynamic forces due to motion, represented by the superscript M, and due to excitation from sinusoidal wakes, represented by the superscript w, are expressed in terms of nondimensional coefficients as follows:

$$L_B^M + L_B^W = -\pi\rho b^3\omega^2 \sum_{r=0}^{N-1} \left[ l_{hhr} \frac{h_{ar}}{b} + l_{har}\alpha_{ar} + l_{whr} \right] e^{i(\omega t + \beta r s)} \quad (8a)$$

$$M_B^M + M_B^W = \pi\rho b^4\omega^2 \sum_{r=0}^{N-1} \left[ l_{ahr} \frac{h_{ar}}{b} + l_{aar}\alpha_{ar} + l_{war} \right] e^{i(\omega t + \beta r s)} \quad (8b)$$

where

$$\begin{aligned} l_{hhr} &= \frac{2i}{k} (C_{Fq})_{\eta} & l_{aar} &= \frac{4}{k^2} (C_{M\alpha})_{\eta} \\ l_{har} &= \frac{2}{k^2} (C_{F\alpha})_{\eta} & l_{war} &= \frac{-4w_r}{k^2v} (C_{Mw})_{\eta} \\ l_{whr} &= \frac{-2w_r(C_{Fw})_{\eta}}{k^2v} & k &= \frac{\omega b}{v} \\ l_{ahr} &= \frac{4i}{k} (C_{Mq})_{\eta} \end{aligned} \quad (9)$$

The coefficients  $(C_{Fq})_{\eta}$ ,  $(C_{F\alpha})_{\eta}$ , ...  $(C_{Mw})_{\eta}$  are calculated by the unsteady cascade airfoil theory of reference 12 for given values of  $k$ ,  $b$ ,  $s/c$ ,  $\xi$ , and  $a (=2\eta - 1)$ . The quantity  $w_r$  is the amplitude of the velocity of the sinusoidal wake in the  $r$ th mode. Nondimensionalizing equation (7), extending the resultant equation to all the blades ( $s = 0, 1, 2 \dots N-1$ ), and using equation (3), the equations for all the blades of a randomly mistuned cascade can be simplified as

$$[[P] - [I]\gamma]\{Y\} = -[E]^{-1}[G][E]\{AD\} \quad (10)$$

where

$$\begin{aligned} [P] &= [[E]^{-1}[D][E] + [E]^{-1}[G][E][A]] \\ [D] &= \begin{bmatrix} [D_0] & & \\ & [D_1] & \\ & & \ddots \\ & & & [D_{N-1}] \end{bmatrix} & G_{Kh_B} &= \mu_s \gamma_{h_B}^2 (1 + 2i\zeta_{h_B}) \\ & & G_{K\alpha_B} &= \mu_s r_{\alpha_B}^2 \gamma_{\alpha_B}^2 (1 + 2i\zeta_{\alpha_B}) \\ [G] &= \begin{bmatrix} [G_0] & & \\ & [G_1] & \\ & & \ddots \\ & & & [G_{N-1}] \end{bmatrix} & \gamma_{h_B} &= \omega_{h_B} / \omega_0 \\ & & \gamma_{\alpha_B} &= \omega_{\alpha_B} / \omega_0 \end{aligned} \quad (11)$$

(Cont'd.)

$$\begin{aligned} [A] &= \begin{bmatrix} [A_0] & & \\ & [A_1] & \\ & & \ddots \\ & & & [A_{N-1}] \end{bmatrix} & \mu_B &= m_B / \pi\rho b^2 \\ [AD] &= [[AD_0][AD_1] \dots [AD_{N-1}]]^T & r_{\alpha_B} &= r_{\alpha_B} / m_B b^2 \\ [D_B] &= \mu_B \begin{bmatrix} 1/G_{Kh_B} & x_{\alpha_B}/G_{Kh_B} \\ x_{\alpha_B}/G_{K\alpha_B} & r_{\alpha_B}^2/G_{K\alpha_B} \end{bmatrix} & x_{\alpha_B} &= s_{\alpha_B} / m_B b \\ & & \gamma &= (\omega_0/\omega)^2 \\ [A_r] &= \begin{bmatrix} l_{hhr} & l_{har} \\ l_{ahr} & l_{aar} \end{bmatrix} \\ [AD_r] &= \begin{bmatrix} l_{whr} & l_{war} \end{bmatrix}^T \\ [G_B] &= \begin{bmatrix} 1/G_{h_B} & 0 \\ 0 & 1/G_{\alpha_B} \end{bmatrix} \end{aligned} \quad (11) \text{ (conc.)}$$

### III. Solution

The aeroelastic stability of the cascade is determined by eigenvalues,  $\gamma^r$ s, of the matrix  $[P]$ . The relation between the frequency  $\omega$  and  $\gamma$  is

$$i\omega/\omega_0 = 1/\sqrt{\gamma} = \bar{\mu} \pm i\bar{v} \quad (12)$$

Flutter occurs when  $\bar{\mu} > 0$ .

For the given values of the number of blades, and hence the allowable interblade phase angles, the gap to chord ratio, the stagger angle, the elastic axis position, and the structural parameters, the eigenvalues of the matrix  $[P]$  are calculated for a range of values of  $k$ . Denoting the values of  $k$  and  $v$  at which  $\bar{\mu} = 0$  as  $k_F$  and  $\bar{v}_F$ , respectively, the nondimensional flutter speed can be written as

$$v_F/b\omega_0 = \bar{v}_F/k_F \quad (13)$$

The aeroelastic response of the blades induced by wakes is calculated from equation (10) and is

$$\{Y\} = -[[P] - [I]\gamma]^{-1}[E]^{-1}[G][E]\{AD\} \quad (14)$$

The amplitude of each blade is obtained by substituting equation (14) into equation (3).

### IV. Results and Discussion

#### A. Computer Program and Verification

A digital computer program was written to calculate the flutter stability boundaries and the blade response of a randomly mistuned rotor. In

this program, it is possible to consider any type of mistuning such as blade-to-blade variations of the uncoupled bending and torsional frequencies, damping ratios, mass ratios, elastic axis and center of gravity positions, and so on. This program is operational on the NASA Lewis Research Center IBM 370/3033. Both tuned and mistuned uncoupled bending and uncoupled torsion cases, in addition to the tuned coupled bending-torsion case, can be treated as special cases of this program. This program was checked for the following special cases:

1. The correctness of the aerodynamic coefficients was checked by comparison of the present results to Whitehead's published results in reference 12 over a wide range of cascade parameters. This comparison shows excellent agreement.

2. To check the correctness of the uncoupled torsional eigenvalues calculated by the present program, a 12-bladed rotor described by Whitehead in reference 3 was considered. The root locus of this rotor with mistuned blades was presented by Whitehead in figure 18 of reference 3. A comparison of the results shows excellent agreement except for the case of zero interblade phase angle. This difference appears to be a plotting error in reference 3 because the present results are also in agreement with those of reference 7 for all interblade phase angles.

3. To check the correctness of the program in calculating the coupled bending-torsion flutter speed of a tuned rotor, the present results for a few selected cases were compared to the corresponding ones in reference 11. This comparison shows excellent agreement.

4. Forced response results are very limited in the published literature. However, an upper-bound for uncoupled bending or torsional response was given in reference 4. The results of the present program are within that bound.

## B. Aeroelastic Stability

A compressor stage representative of a forward stage of an advanced axial flow compressor was chosen for conducting parametric studies. This stage, known as the NASA Test Rotor 12, is shown in figure 3. The required parameters of this stage were calculated from the data given in reference 20 and are listed in table 1. The blade bending to torsion frequency ratio for this rotor is 0.357, and the elastic axis and C.G. position are at 50 percent chord. As a result, the coupling between bending and torsion is very weak and the flutter mode is dominated by torsional motion. Hence, the results for the predominantly bending modes for some cases will not be presented. However, to conduct parametric studies the bending to torsion frequency ratio and elastic axis position are varied. For these cases the results for predominantly bending modes are included. In some selected cases only uncoupled torsional motion is considered.

A comparison of the system eigenvalues of both tuned and mistuned cascades is useful to understand the mistuning effects. For example, figure 4 is such a plot for a special case in which only uncoupled torsional motion of the blades is considered. The first type of mistuning considered is

the one in which the odd and even numbered blades have different torsional frequencies. This is known as alternate blade mistuning. For example, in the case of one percent mistuning, the frequency ratio  $\omega_{\alpha_n}/\omega_0$  is 1.005 for all the even blades and is 0.995 for all the odd blades. The reference frequency  $\omega_0$  is equal to the arithmetic mean of the uncoupled torsional frequencies of all the blades. Because of the symmetry of this type of mistuning the  $\beta_r$  mode couples with the  $(\beta_r + \pi)$  mode only. Figure 4 may be viewed as a root locus for the tuned cascade with  $\beta_r$  as the parameter. When the blades are mistuned, this description is not completely appropriate because each mode contains all possible interblade phase angles. Due to the inherent symmetry in alternate blade mistuning, each mistuned mode contains only two interblade phase angle modes. However, one can view this plot as a root locus with a predominant interblade phase angle as a parameter. Several interesting observations follow from figure 4. Even one percent of mistuning significantly affected the system eigenvalues and stabilized an unstable tuned cascade. As the level of mistuning is increased, the horizontal width of the root locus is decreased. This amounts to saying that the effective damping of some modes is increased while that of others is decreased. This behavior will have an influence on forced response which will be discussed later. When the mistuning level is 1.5 percent, the root locus is split into high and low frequency groups. In the high frequency group all the interblade phase angles between 0 and 90 and between 276.4 and 360 are predominant; in the low frequency group those between 96.4° and 270° are predominant. As the level of mistuning is increased beyond 1.5 percent, the frequency separation of these groups becomes larger and the area enclosed by each group decreases.

Figure 5 shows the eigenvector corresponding to the least stable point of the 1.5 percent mistuning curve on figure 4. The predominant interblade phase angle at this point is 51.42° ( $r = 8$ ) and is coupled with 231.42° mode ( $r = 36$ ). As can be seen, all the even blades have the same amplitude and all the odd blades have the same amplitude, as expected from the symmetry of this kind of mistuning. However, the amplitude of the odd blades is 68 percent of that of even blades.

Figure 6 illustrates the variation of uncoupled flutter speed with the level of alternating blade mistuning with and without damping. The value of the damping ratio used is 0.2 percent and is the same for all the blades. The results indicate that the mistuning has a substantial effect on flutter speed. For the undamped case, the flutter speed increases monotonically with increase in mistuning level. However, when the mistuning level is 5 percent and more, the additional benefit is modest. For the damped case a similar variation in flutter speed is noticed, except when the mistuning is between 0-1 percent. In this range, the damping effect is more pronounced. It should be noted that these observations, particularly the effects of mistuning, are in agreement with the qualitative conclusions analytically reached in reference 4 and the experimental results reported in reference 21.

A second, more common type of mistuning was analyzed. Blade torsional frequencies were randomly chosen from a normally distributed population with a mean  $\omega_{\alpha_n}/\omega_0$  of 1 and a standard deviation

of 0.005. The resulting blade frequencies are shown in figure 7. A comparison of both the tuned and mistuned eigenvalues is shown in figure 8. The tuned eigenvalues are the same as those presented in figure 4. As can be seen, there is stabilizing effect on the system, but is not quite as strong as that produced by one percent alternating mistuning shown in figure 4. The eigenvector for the least stable mistuned mode from figure 8 is shown in figure 9. The eigenvector consists predominantly of  $64.29^\circ$  interblade phase angle mode but also has significant participation from the  $57.86^\circ$ ,  $83.57^\circ$ ,  $19.29^\circ$  and  $77.14^\circ$  modes. Also, each blade has a different amplitude and the interblade phase angle varies considerably. It can be seen that this flutter mode can be viewed as a localized phenomena since only blades numbered 42 through 51 have large relative amplitudes. This type of behavior has been observed in actual engine tests.

The effect of elastic axis position on flutter speed is of interest. Both uncoupled torsional and coupled bending-torsion flutter analyses were formed with and without damping for three elastic axis positions with the center of gravity at mid-chord. As was noticed in reference 11, very weak instabilities appeared in some cases which were eliminated by the addition of a small amount of structural damping. Consequently, they are of little practical interest, and, hence, only the results with structural damping are presented in figure 10. Note, that for uncoupled torsional flutter the worst location of the elastic axis is at the midchord point ( $a = 0$ ). This is in contrast to the present results without damping and to those in references 9 and 11 in which a severe drop in flutter speed is noticed for the 75 percent elastic axis position. For coupled bending-torsion flutter, the effect of elastic axis position depends on  $\omega_{h_0}/\omega_0$ . If  $\omega_{h_0}/\omega_0 = 1$ , the best location (of the three locations investigated herein) is the 75 percent chord point; if  $\omega_{h_0}/\omega_0 \gg 1$ , the best location is the 25 percent chord point. When the elastic axis is off the midchord, the effect of bending-torsion coupling on flutter speed is significant. This observation is in agreement with that in references 5 and 11. These results suggest that the tailoring of the elastic axis position can be used as a passive control to increase flutter speed as is done in fixed wing aeroelasticity.

Figure 11 shows the effects of both alternating blade mistuning and damping on coupled bending-torsion flutter speed. As can be seen, both mistuning and damping have beneficial effects. However, the level of benefit depends on  $\omega_{h_0}/\omega_0$ . It should be noted that the adverse effect of coupling between bending and torsion i. e. tuned cascade flutter speed when  $\omega_{h_0}/\omega_0 = 1$  is reduced by the beneficial effect of small mistuning and/or damping.

The effects of alternating blade mistuning, damping, and elastic axis position on the coupled bending torsion flutter speed are illustrated in figure 12. The effects of mistuning and damping are similar to those discussed in figure 6; the effects of the elastic axis position are similar to those discussed in figure 10. For all practical purposes, the curves for the elastic axis at mid-chord are the same as those in figure 6 because the ratio  $\omega_{h_0}/\omega_0 (=0.357)$  is small.

The results presented thus far only show the effects of mistuning on aeroelastic stability. These results suggest that the utilization of mistuning and/or tailoring of the elastic axis position as passive controls to increase flutter speed are feasible. The next step is to examine the effect of mistuning on forced response.

### C. Aeroelastic Response

In the present formulation, it is possible to consider an excitation function consisting of all harmonics of rotational speed of the rotor which range up to  $r = N-1$ . In engine aeroelastic terminology, the harmonic number  $r$  is known as the 'engine order' of the excitation. The coefficients  $\lambda_{whr}$  and  $\lambda_{war}$  in equations 8(a) and (b) represent the forcing functions in the bending and torsion equations, respectively. To understand the nature of the response, excitation in only one harmonic at a time will be considered. This results in no loss of generality since the principle of superposition holds. If the  $r = R$  harmonic is considered, then the column matrices  $\{AD_0\}$ ,  $\{AD_1\}$ , ...,  $\{AD_{N-1}\}$  are zero except  $\{AD_R\}$  in equation (11). This corresponds to the case in which there are  $R$  asymmetrically spaced obstructions located upstream from the blades and the circumferential wake distribution is perfectly sinusoidal. For practical applications, the forcing frequency is thus equal to  $R$  times the rotational speed.

The aeroelastic response results presented herein are for two values of  $R$ , 11 and 39, at a fixed reduced frequency chosen such that the cascade is aeroelastically stable in all modes. These values for  $R$  were picked because the aerodynamic damping of the tuned system in the  $r = 11$  mode is relatively low whereas that in the  $r = 39$  mode is relatively high. The forcing frequency range investigated is limited to a small range around the uncoupled torsional frequency.

If the blades are tuned, the response will be entirely in the  $r = R$  mode, and all the blades have equal amplitude. The amplitude of response of any blade is  $\begin{Bmatrix} h_a \\ \alpha_a \end{Bmatrix}$  which is a function of  $\omega/\omega_0$ .

Let the torsional amplitude of resonance of each blade of the tuned rotor be  $\alpha_{0,1d}$ . If the blades are now randomly mistuned, there will be a response in all the modes (enumerated by  $r$ ) and the amplitude of response of the  $a$ th blade is

$$\begin{Bmatrix} h_a \\ \alpha_a \end{Bmatrix} = \sum_{r=0}^{N-1} \begin{Bmatrix} h_{ar} \\ \alpha_{ar} \end{Bmatrix} e^{i\beta_r a} \quad (15)$$

Figures 13(a) and (b) with  $R = 11$ , and figures 13(c) and (d) with  $R = 39$  show the variation of  $\alpha_a/\alpha_{0,1d}$  for both the tuned and one percent alternating blade mistuned cascades. Note that figures 13(b) and (d) are a repetition of figures 13(a) and (c), respectively, with 0.2 percent structural damping. Note that the torsional amplitude  $\alpha_{0,1d}$  of the tuned cascade depends on the level of damping and  $R$ . The bending amplitudes are not shown because they are very small in the range of the excitation frequency shown herein. For the alternating blade mistuning, only two  $r$  modes are coupled. The

amplitude behavior is similar to that shown in figure 5 in which the amplitudes of the odd and even blades are different. In all these cases, the single resonance peak of the tuned cascade is replaced by twin resonance peaks for the alternating mistuned cascade. It is seen that the effect of mistuning on forced response depends on the engine order of the forcing function. For example, the mistuning has a beneficial effect (fig. 13(a)) on torsional response for  $R = 11$ , but has an adverse effect (fig. 13(c)) for  $R = 39$ . This is in contrast to the common belief that the mistuning always has an adverse effect on forced response. Thus, this result provides an added incentive for pursuing the use of mistuning as a passive control. The maximum decrease in amplitude with mistuning for  $R = 11$  is approximately 85 percent (fig. 13(a)) without damping and is approximately 25 percent (fig. 13(b)) with damping. The maximum increase in amplitude with mistuning for  $R = 39$  is approximately 110 percent without damping and is approximately 40 percent with damping. As expected, the structural damping has a significant effect on forced response. Although not shown, the decrease in tuned resonance response is 91 percent for  $R = 11$  and 37 percent for  $R = 39$ .

The randomly mistuned cascade described in figure 7 was analyzed for forced response with  $k = 1.2$ . The results are shown in figures 14(a) for  $R = 11$  and 14(b) for  $R = 39$ . As in figure 9, each blade has a different amplitude and the interblade phase angle varies. It is seen that the single resonance peak for the tuned case is changed into multiple peaks, and different blades peak at different forcing frequencies. As in the alternating mistuning case, this type of mistuning has a beneficial effect on the  $R = 11$  excitation. For the  $R = 39$  excitation, the sharp resonance peak of the tuned system is eliminated. However, for most of the values of the forcing frequency, the mistuned response is higher than the tuned response.

#### V. Conclusions

This investigation was conducted in an attempt to improve the basic understanding of the effects of mistuning on aeroelastic stability and response and then to explore the feasibility of using mistuning as a passive control to increase flutter speed and to minimize response. The following conclusions are reached on the basis of the limited results obtained by using incompressible unsteady cascade aerodynamic theory for two types of mistuning:

1. In general, the mistuning has a beneficial effect on the coupled bending-torsion flutter speed. The flutter speed increases monotonically with an increase in alternating blade mistuning level. However, when the mistuning level is above about 5 percent and more, the additional benefit is modest.

2. The inherent random mistuning which exists in real fan, compressor, and turbine stages has a significantly beneficial effect on flutter. This observation is qualitatively in agreement with the experimental results published in the literature.

3. As expected, the effect of structural damping on flutter speed is stabilizing. However, in the presence of mistuning this effect is not as significant as in the tuned case.

4. The use of uncoupled torsional flutter analysis to deduce the effect of elastic axis positioning was found to be unreliable because the coupling between bending and torsion, structural damping, and mistuning can change the results significantly.

5. Mistuning may have either a beneficial or an adverse effect on forced response, depending on the engine order of excitation.

6. Mistuning introduced multiple resonant peaks for a given engine order excitation.

#### References

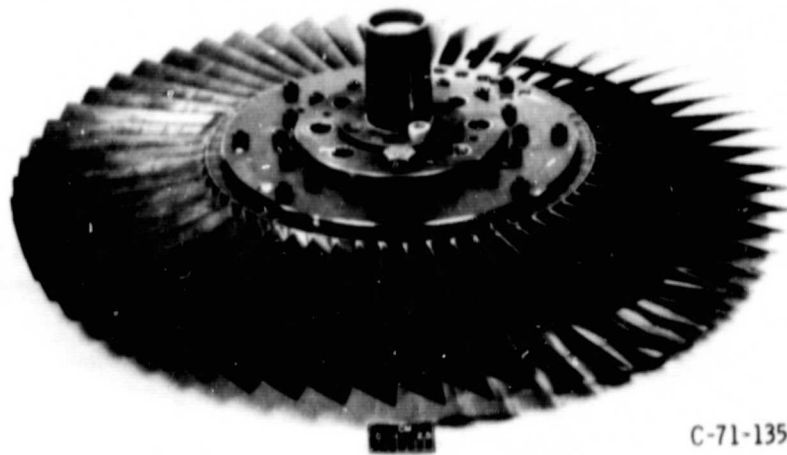
1. Cardinale, J. M., Bankhead, H. R., and McKay, R. A., "Experimental Verification of Turboblading Aeromechanics," presented in the AGARD 56th Symposium on Turbine Engine Testing, Torino, Italy, Sept. 29-Oct. 3, 1980.
2. Srinivasan, A. V., and Fryo, H. M., "Effects of Mistuning on Resonant Stresses of Turbine Blades," paper presented at the Winter Annual Meeting of the American Society of Mechanical Engineers, New York, New York, Dec. 5-10, 1976.
3. Whitehead, D. S., "Torsional Flutter of Unstalled Cascade Blades at Zero Deflection," R&M 3429, 1965 (CAT Memo 12/63, ARC 26085).
4. Whitehead, D. S., "Effect of Mistuning on the Vibration of Turbomachine Blades Induced by Wakes," Journal of Mechanical Engineering Science, Vol. 8, No. 1, 1966, pp. 15-21.
5. Hanamura, Y. and Tanaka, H., "A Modification of Flutter Characteristics by Changing Elastic Nature of Neighboring Blades in Cascades," paper No. 50, presented at 1977 Tokyo Joint Gas Turbine Congress held in Japan, May 22-27, 1977.
6. Ewins, D. J., "An Experimental Investigation of the Forced Vibration of Bladed Disks due to Aerodynamic Excitation," paper presented at the Winter Annual Meeting of the American Society of Mechanical Engineers, New York, New York, Dec. 5-10, 1976.
7. Srinivasan, A. V., "Influence of Mistuning on Blade Torsional Flutter," NASA CR-165137, Aug. 1980.
8. Shiori, J., "Non-Stall Normal Mode Flutter in Annular Cascades, Part II - Experimental Study," Transactions of Japan Society of Aeronautical Engineering, Vol. 1, p. 26, 1958.
9. Carta, F. O., "Coupled Blade-Disk-Shroud Flutter Instabilities in Turbo-jet Engine Rotors," Journal of Engineering for Power, 1967, pp. 419-426.
10. Rao, B. M. and Kronenburger, L., Jr., "Aeroelastic Characteristics of a Cascade of Blades," Texas A&M Res. Foundation, College Station, Texas, Report No. AFOSR-TR-78-1027 (Feb. 1978), AD-A055 619/IGA.
11. Bendikson, O. and Friedman, P., "Coupled Bending-Torsion Flutter in Cascades," AIAA Journal, Vol. 18, No. 2., Feb. 1980, pp. 194-201.

12. Whitehead, D. G., "Force and Moment Coefficients for Vibrating Airfoils in Cascades," R&M 3254, British Aeronautical Research Council, London, Feb. 1960.
13. Smith G. G. G., and Eichuri, V., "Aeroelastic and Dynamic Finite Element Analysis of a Bladed Shrouded Disk," N. S. CR-159728, March 1980.
14. Kislak, R. E., and Kaza, K. R. V., "Aeroelastic Characteristics of a Cascade of Mistuned Blades in Subsonic and Supersonic Flows," paper to be presented at the 8th Biennial AGME Engineering Division Conference on Mechanical Vibration and Noise, Hartford, Conn., Sept. 20-23, 1981.
15. Lane, P., "System Mode Shapes in the Flutter of Compressor Blade Rows," Journal of the Aeronautical Sciences, Vol. 23, No. 1, Jan. 1956, pp. 54-56.
16. Dugundji, J., "Flutter Analysis of a Tuned Rotor with Rigid and Flexible Disks," GT&PDL Report No. 146, M.I.T., Cambridge, Mass., July 1979.
17. Bisplinghoff, R. L., and Ashley, H., "Principles of Aeroelasticity," John Wiley and Sons, Inc., New York, 1962.
18. Smith, S. N., "Discrete Frequency Sound Generation in Axial Flow Turbomachines," A.R.C. R&M No. 3709, 1973.
19. Adamczyk, J. J., and Goldstein, M. E., "Unsteady Flow in a Supersonic Cascade with Subsonic Leading Edge Locus," AIAA Journal, Vol. 16, No. 12, December 1978, pp. 1248-1254.
20. Moore, D. R., and Reid, R., "Performance of a Single-Stage Axial-Flow Transonic Compressor Stage with a Blade Tip Solidity of 1.7," NASA TM X-2658, December 1972.
21. Nabatova, N. A., and Shipov, R. A., "Influence of the Material of the Rotor Blades of an Axial-Flow Compressor under Flutter Initiating Conditions," translated from Problemy-Prochnosti, No. 8, pp. 63-67, Aug. 1974.

Table 1 Parameters of NASA Test Rotor 12

N	56
b/c	0.534
$\mu_B$	258.5
a	0 (varied in some cases)
$x_{10}$	0 (varied in some cases)
$r_{10}$	$\left\{ \begin{array}{l} 0.5774 \text{ (} a = 0 \text{)} \\ 0.7638 \text{ (} a = -0.5 \text{ and } 0.5 \text{)} \end{array} \right.$
$\xi$	$34.4^\circ$
$\omega_{h0}/\omega_{d0}$ (tuned)	0.357 (varied in some cases)





C-71-1356

Figure 3. - NASA test Rotor 12.

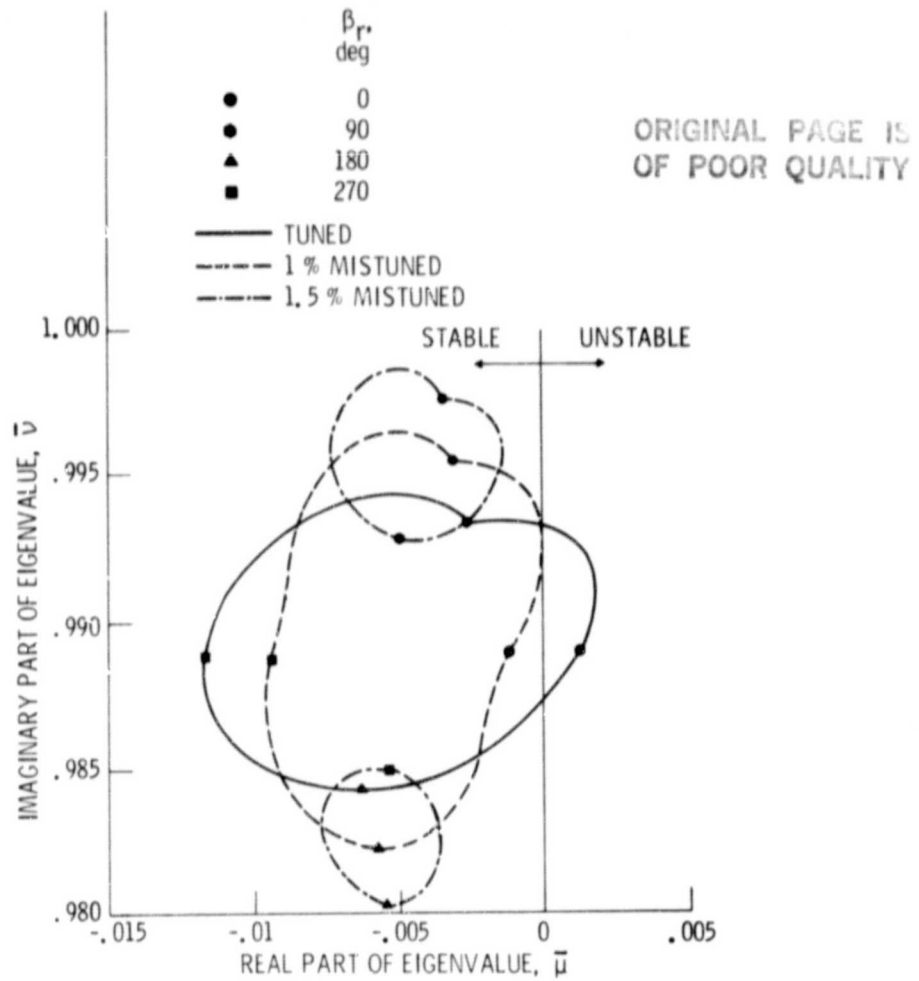


Figure 4. - Effect of alternating blade mistuning on eigenvalues (torsion only):  $a = 0$ ,  $k = 0.642$ ,  $\zeta_{h_s} = \zeta_{a_s} = 0$ .

ORIGINAL PAGE  
OF POOR QUALITY

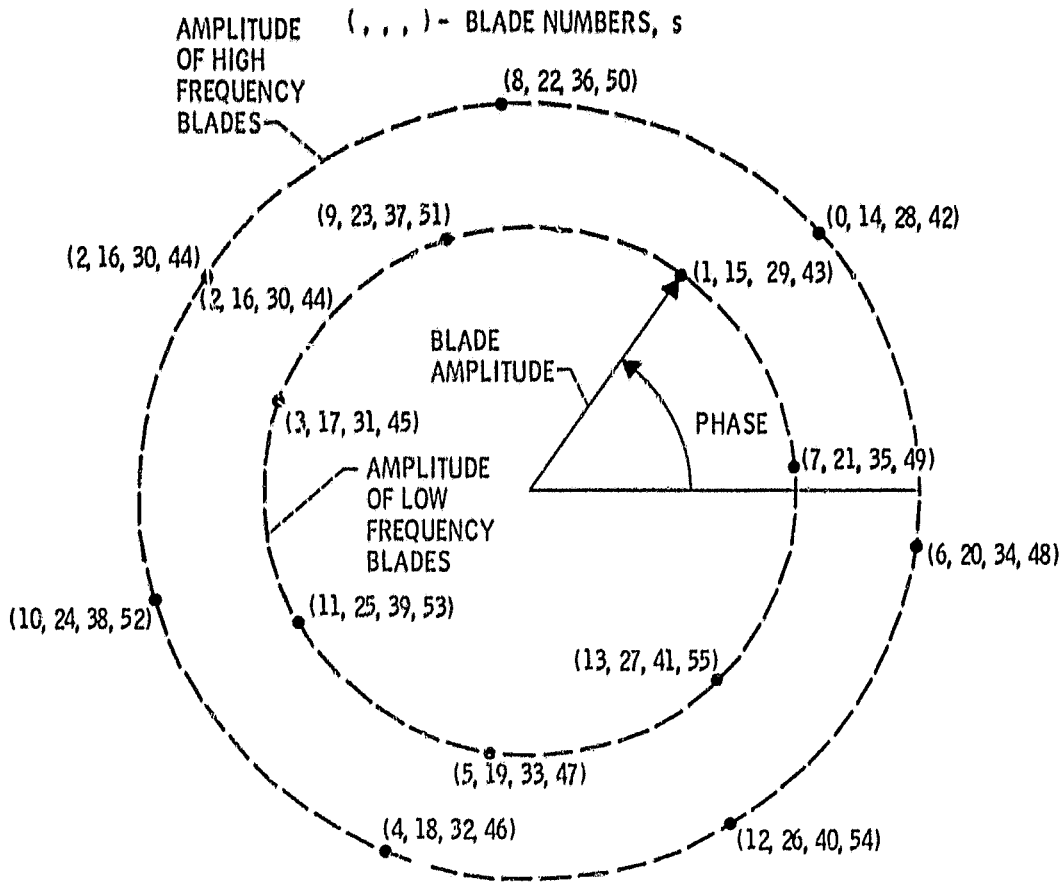


Figure 5. - Effect of alternating blade mistuning on the eigenvector of the least stable eigenvalue from Figure 4 with 1 % mistuning.

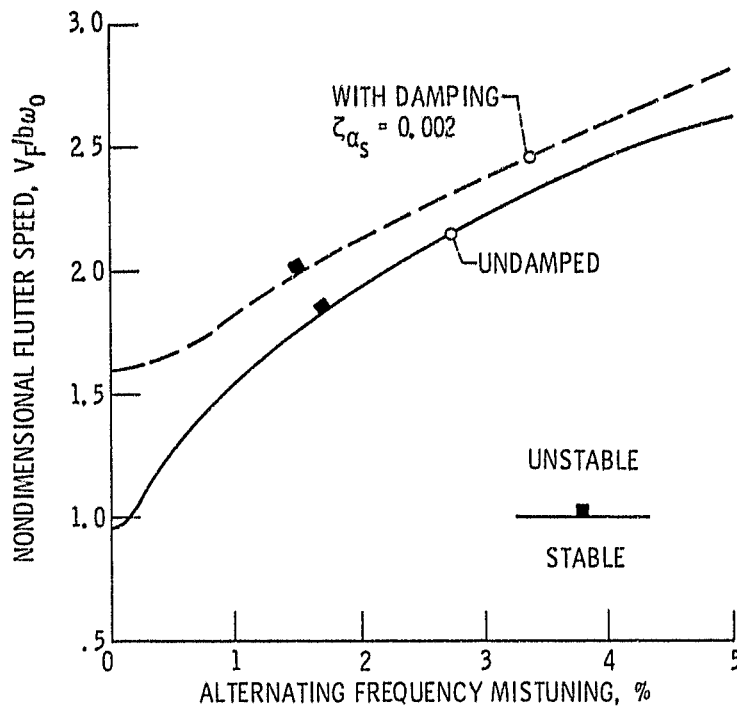


Figure 6. - Variation of uncoupled torsional flutter speed with alternating blade mistuning both with and without damping;  $\alpha = 0$ .

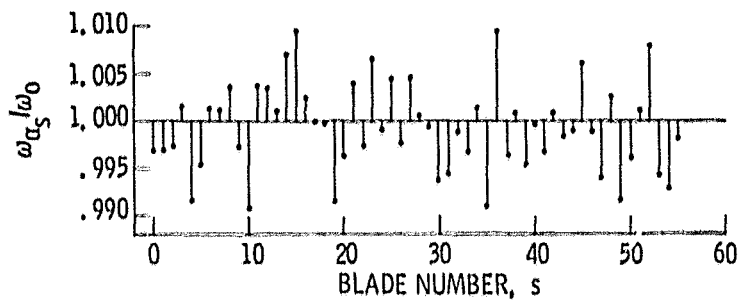


Figure 7. - Individual blade torsional frequencies for the randomly mistuned case.

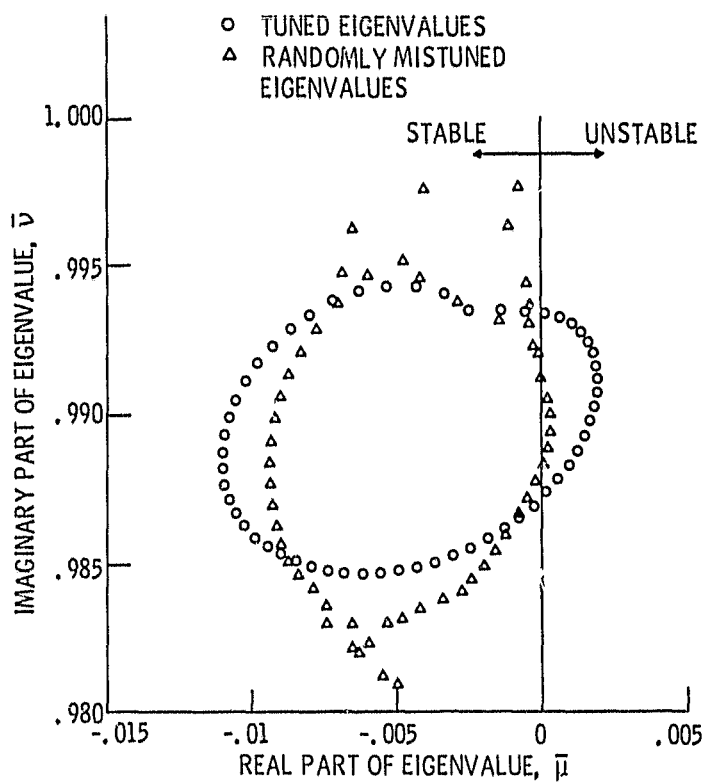


Figure 8. - Effect of random mistuning on eigenvalues (torsion only);  $a = 0$ ,  $k = 0.642$ ,  $\zeta_{h_s} = \zeta_{\alpha_s} = 0$ .

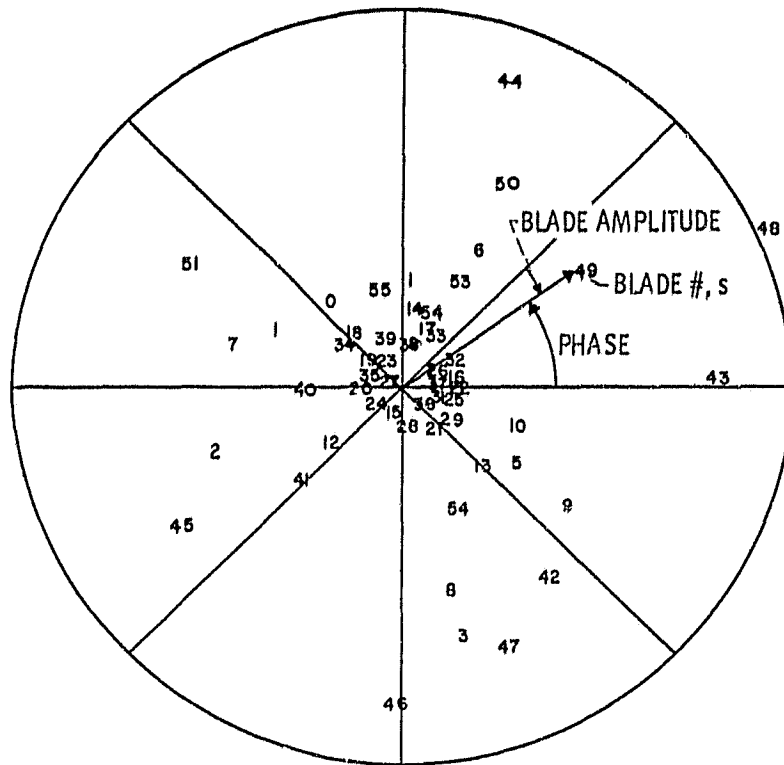
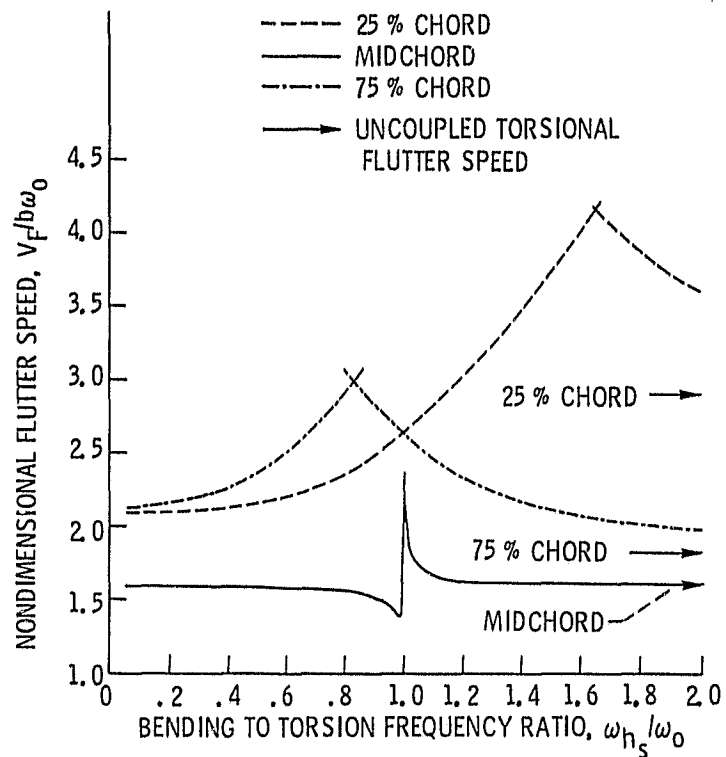


Figure 9. - Effect of random mistuning on the eigenvector of the least stable eigenvalues from Figure 8.



ORIGINAL PAGE IS  
OF POOR QUALITY

Figure 10. - Effect of bending-torsion coupling on flutter speed;  $\zeta_{h_s} = \zeta_{a_s} = 0.002$ , c.g. at midchord.

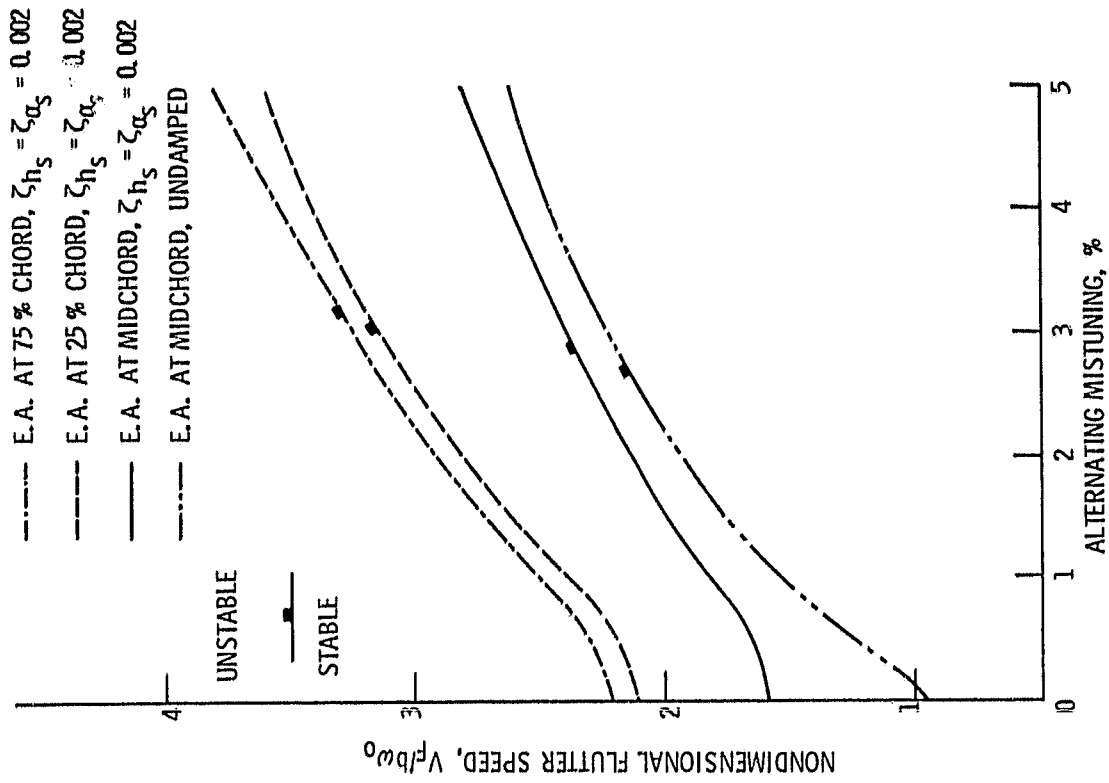


Figure 12. - Variation of coupled bending-torsion flutter speed with mistuning;  $\omega_{h_s}/\omega_0 = 0.357$ , c.g. at midchord.

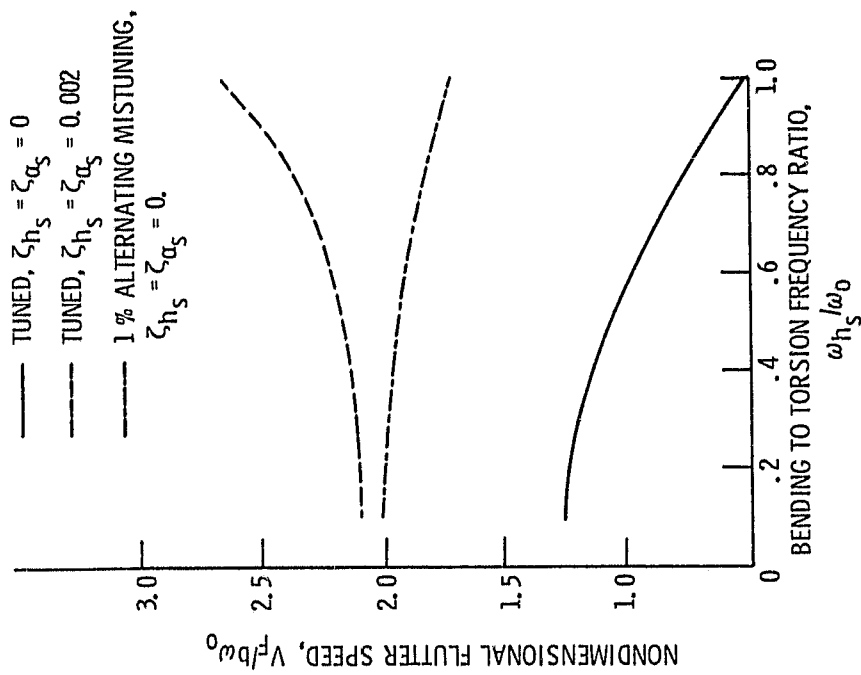


Figure 11. - Effect of mistuning and structural damping on coupled bending-torsion flutter;  $a = -0.5$ , c.g. at midchord.

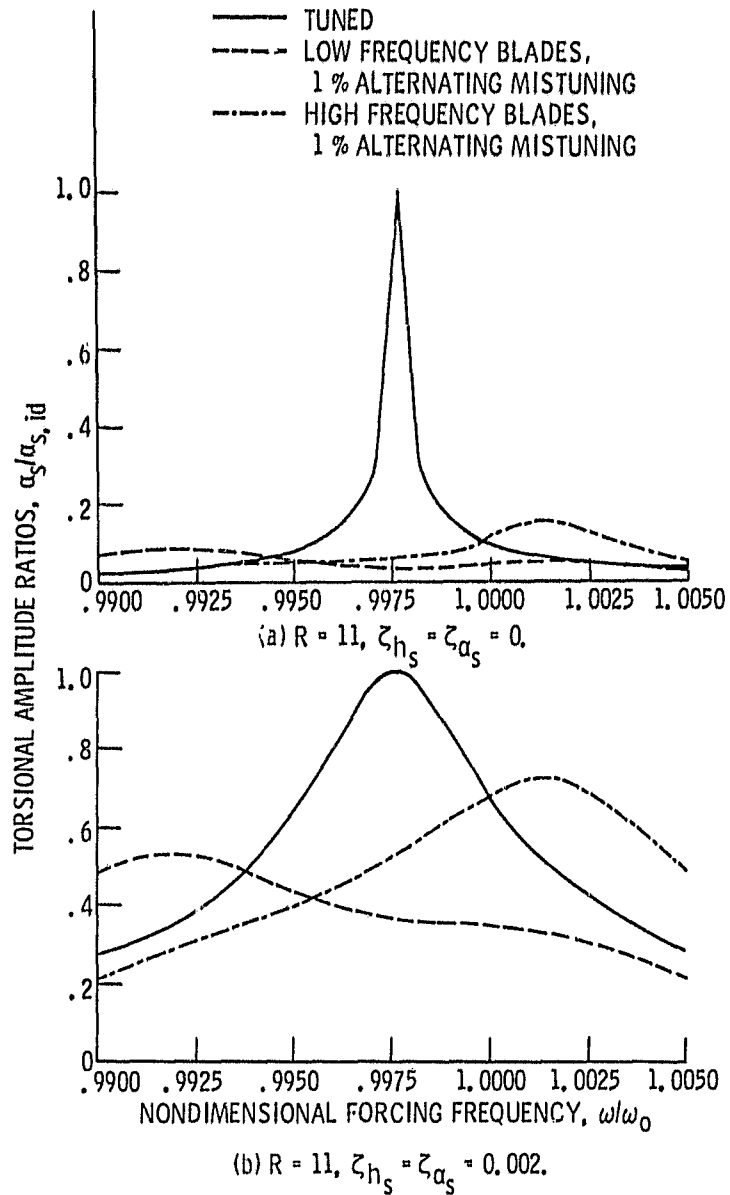


Figure 13. - Effect of blade alternating mistuning on coupled bending torsional response;  $a = 0$ ,  $\omega_{h_s} / \omega_0 = 0.357$ ,  $k = 1.2$ , c.g. at midchord.

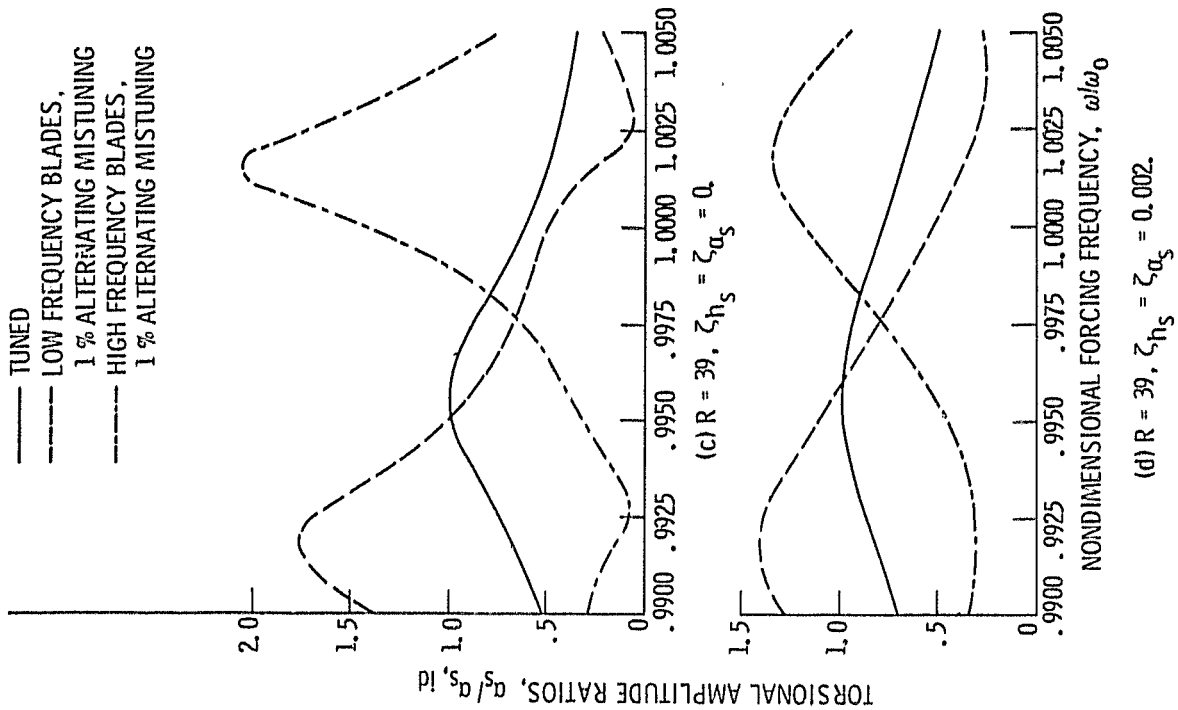


Figure 13. - Concluded.

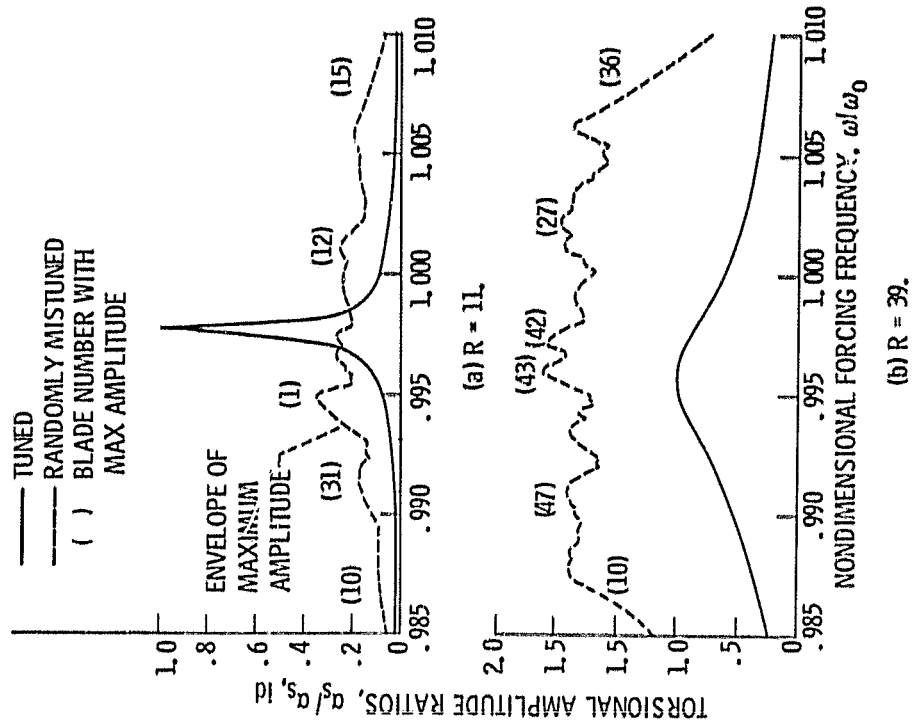


Figure 14. - Effect of blade random mistuning on coupled bending-torsion response;  $a = 0, \omega_{h_s}/\omega_0 = 0.357, c.g.$  at midchord,  $\zeta_{h_s} = \zeta_{\alpha_s} = 0, k = 1.2$ .

1. Report No NASA TM-81674	2. Government Accession No.	3. Recipient's Catalog No	
4. Title and Subtitle EFFECTS OF MISTUNING ON BENDING-TORSION FLUTTER AND RESPONSE OF A CASCADE IN INCOMPRESSIBLE FLOW		5. Report Date	
		6. Performing Organization Code 505-33-82	
7. Author(s) Krishna Rao V. Kaza, The University of Toledo, Toledo, Ohio, and Robert E. Kielb, Lewis Research Center		8. Performing Organization Report No. E-699	
		10. Work Unit No.	
9. Performing Organization Name and Address National Aeronautics and Space Administration Lewis Research Center Cleveland, Ohio 44135		11. Contract or Grant No. NSG-3139	
		13. Type of Report and Period Covered Technical Memorandum	
12. Sponsoring Agency Name and Address U.S. Department of Energy Division of Solar Thermal Energy Systems Washington, D.C. 20545		14. Sponsoring Agency Code Report No. DOE/NASA/1028-29	
		15. Supplementary Notes Prepared under Interagency Agreement EX-76-I-01-1028. Prepared for Dynamics Specialists Conference sponsored by the American Institute of Aeronautics and Astronautics, April 9-11, 1981.	
16. Abstract This paper presents an investigation of the effects of blade mistuning on the aeroelastic stability and response of a cascade in incompressible flow. The aerodynamic, inertial, and structural coupling between the bending and torsional motions of each blade and the aerodynamic coupling between the blades are included in the formulation. A digital computer program was developed to conduct parametric studies. Results indicate that the mistuning has a beneficial effect on the coupled bending-torsion and uncoupled torsion flutter. The effect of mistuning on forced response, however, may be either beneficial or adverse, depending on the engine order of the forcing function. Additionally, the results illustrate that it may be feasible to utilize mistuning as a passive control to increase flutter speed while maintaining forced response at an acceptable level.			
17. Key Words (Suggested by Author(s)) Aeroelasticity Flutter Forced response Mistuning		18. Distribution Statement Unclassified - unlimited STAR Category 39 DOE Category UC-96	
19. Security Classif. (of this report) Unclassified	20. Security Classif. (of this page) Unclassified	21. No. of Pages	22. Price*